Effect of Spatial Confinement on the Morphology Evolution of Thin Poly(*p*-phenylenevinylene)/Methanofullerene Composite Films

Xiaoniu Yang,[†,⊥] Alexander Alexeev,[‡,#] Matthias A. J. Michels,[†,⊥] and Joachim Loos[*,‡,§,⊥]

Group Polymer Physics, Laboratory of Materials and Interface Chemistry, and Laboratory of Polymer Technology, Eindhoven University of Technology, P.O. Box 513, NL-5600 MB Eindhoven, The Netherlands; Dutch Polymer Institute, P.O. Box 902, NL-5600 AX Eindhoven, The Netherlands; and NT-MDT, 124460 Moscow, Russia

Received November 22, 2004; Revised Manuscript Received March 7, 2005

ABSTRACT: The morphology evolution of poly(*p*-phenylenevinylene)/methanofullerene (MDMO-PPV/PCBM) composite films as used for photovoltaic devices has been investigated upon thermal annealing under various spatial confinements. Three types of spatial confinement have been studied: no confinement, which corresponds to free-standing composite films; single-sided confinement, in which the composite films are deposited on a substrate; and double-sided or sandwich-like confinement, in which the deposited composite films are additionally covered by a top layer. For all the confinement types, annealing above the glass transition temperature T_g of bulk MDMO-PPV forces crystallization of PCBM molecules into single crystals from the MDMO-PPV matrix and causes phase separation. The mobility of PCBM molecules in the MDMO-PPV matrix and its crystal growth rates decrease with increased degree of confinement. In the case of free-standing films the diffusion rate of PCBM is so high that the molecule incorporation rate at the growing front of the PCBM crystals determines their growth rate; elongated single crystals are formed due to the anisotropy of the crystal growth in the lateral dimensions. For single- and double-sided confinement, the mobility of PCBM is lower, and in particular for double-sided confinement, diffusion instead of incorporation rate of PCBM molecules dominates crystal growth, which results in less elongated (single-sided confinement) and even circular (double-sided confinement) shapes of the single crystals formed. Therefore, spatial confinement reduces the mobility of PCBM molecules and thus its crystallization kinetics in its thin composite films.

Introduction

Recently, thermal treatment has successfully been employed to improve the performance of bulk heterojunction plastic photovoltaic cells based on dye/polymer,[1−3] fullerene/polymer,[4] or low-molecular-weight organic thin composite films serving as photoactive layer.[5] Annealing can be performed either during[3] or after[1,2,4,5] device fabrication. For the former case, the active film is annealed just after deposition on a substrate, most time a glass slide coated with thin layers of indium tin oxide (ITO) and poly(ethylenedioxythiophene):poly(styrenesulfonate) (PEDOT:PSS), but before evaporation of the top metal contact layer; the composite film is annealed in the condition of single-sided confinement. This method has specific advantages since stress release will happen at the free surface of the film, and contact damage[6] at the interface between the active layer and the top metal layer during annealing can be avoided. For the latter case, the annealing treatment of the active layer is conducted after the evaporation of top metal layer and hence in a double-sided confined condition.

Another aspect of annealing treatments is to investigate the thermal stability of active layers[7,8] or entire devices.[9] In the previous studies, [6,6]-phenyl C_{61} butyric acid methyl ester (PCBM) segregates and forms large crystals within thin poly(*p*-phenylenevinylene)/methanofullerene (MDMO-PPV/PCBM) composite films upon annealing in both free-standing[7] and substrate-supported[8] conditions have been demonstrated. Even for temperatures below the glass transition temperature T_g of the surrounding polymer in bulk, large-scale crystallization of PCBM has been observed. The mobility of PCBM is interpreted as coupling to or being decoupled from various relaxation processes of the polymer molecules within the matrix in the frame of free volume theory.[10,11] Moreover, this characteristic mobility of small molecules in a polymer matrix has been utilized to investigate the segmental motions of polymer molecules occurring near T_g in either the bulk state or thin films[12,13] by applying techniques such as fluorescence quenching,[14] fluorescence recovery after photobleaching,[15] UV−vis and infrared spectroscopy,[16,17] holographic recovery after photobleaching (HFRAP),[18] and fluorescence nonradiative energy transfer (NRET).[19] Organic compounds frequently used for this purpose are dye molecules, due to its easy detection at rather low concentrations.

It has been shown that the dynamics of reorganization of a thin film upon thermal treatment not only is determined by the composition and architecture of the film itself but also depends on its local environment. Numerous experiments indicate that the mobility of polymer molecules in the vicinity of a surface or an interface is perturbed,[20−22] and the extent to which they affect the mobility of polymer chains depends on the strength of their interactions with the surface/interface.

[†] Group Polymer Physics, Eindhoven University of Technology.
[‡] Laboratory of Materials and Interface Chemistry, Eindhoven University of Technology.
[§] Laboratories of Polymer Technology, Eindhoven University of Technology.
[⊥] Dutch Polymer Institute.
[#] NT-MDT.
[*] To whom correspondence should be addressed: e-mail j.loos@tue.nl; Ph (31) 40-2473033.

10.1021/ma047589x CCC: $30.25
Published on Web 04/09/2005

Scheme 1. Device Structure of a Ready-to-Work Plastic Photovoltaic Cell or Light-Emitting Diode, in Which the Active Layer (Thin Composite Film) Is Sandwiched between Two Layers Serving as the Functions of Holes Injection and Electrons Transport

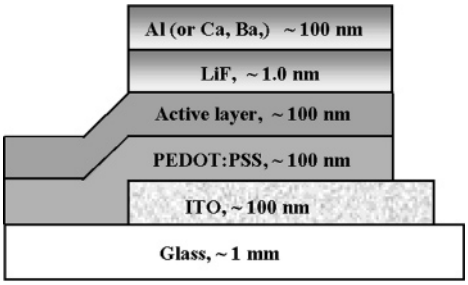

At a free surface, there is a preferential aggregation of chain ends.[23,24] The presence of these chain ends will increase the free volume and consequently enhance the mobility of molecules at the surface. However, experimental studies have yielded contradictory results. For example, it is claimed that the T_g is reduced at the regions close to the surface;[25−28] however, others have found that T_g of the free surface and the bulk is identical.[29,30] Anyway, these results would suggest that the mobility of molecules in the vicinity of a free surface would either remain unchanged or increase. For the case that the thin film is covered and thus an impenetrable interface is created, the situation becomes more complicated. Strong attraction between the two films may retard the mobility of molecules and yields in a reduced diffusion coefficient.[31] In contrast, a weak interaction will hardly affect the mobility of molecules, and in the extreme case even the T_g can be decreased similar as in the case of a free surface.[32]

For a ready-to-work organic optoelectronic device (photovoltaic cells or light-emitting diodes), the active composite film is actually sandwiched between two solid layers: a top metal layer of e.g. Al, LiF/Al, Ca, or Ba and a PEDOT:PSS-coated substrate, as shown in Scheme 1. Therefore, the morphological evolution with time and the thermal stability of the active layer is strongly determined by its interaction with these two interfaces. In the present study, we have investigated the reorganization of photoactive thin MDMO-PPV/PCBM composite films upon annealing for different conditions of spatial confinements: no confinement, which corresponds to free-standing composite films; single-sided confinement, in which one side of the composite films is supported; and double-sided or sandwich-like confinement, in which the composite films are covered on both sides. The main focus of the study is to understand how confinement influences the mobility of PCBM molecules in the thin composite films. The knowledge obtained from this study can be applied to other active composite films, e.g., dye/polymer composites as applied in OLEDs, which somewhat have a similar componential architecture.

Experimental Part

All the thin composite films were prepared based on the standard active layer fabrication method for photovoltaic device as follows. Glass plates fully covered with a 60 nm thick layer of ITO were used as substrates. These substrates were first cleaned by ultrasonic treatment in acetone, followed by rubbing with soap, rinsing in demineralized water, and refluxing with 2-propanol to remove water. The substrates were treated in a UV-ozone oven for ca. 20 min. Subsequently, a layer of ~100 nm poly(ethylenedioxythiophene):poly(styrenesulfonate) (PEDOT:PSS, Bayer AG, Germany) was spin-coated from an aqueous dispersion on the cleaned substrates. This layer was dried by heating on a hot plate at 180 °C for ca. 1 min, followed by cooling on a plate at 25 °C for 1 min.

Mixed solutions for the active composite film deposition were prepared by dissolving PCBM and MDMO-PPV (synthesized via the Gilch route) with MDMO-PPV/PCBM with 80 wt % PCBM, which is the most favorable composition for solar cell applications,[33] in the solvent chlorobenzene and continuously stirring in the dark overnight. The solution was spin-coated on top of the PEDOT:PSS to form the thin composite film. The concentration of the solution and spin-coating parameters were adjusted to yield homogeneous films with thickness around 100 nm. Finally, ~1 nm LiF and subsequently ~100 nm aluminum metal cap were deposited by thermal evaporation in a vacuum chamber (5×10^{-6} mbar, 1 ppm of O_2 and <1 ppm of H_2O). The samples were rotated at ~1 Hz during deposition to guarantee homogeneous films. Following these procedures ready-to-work devices were obtained. These devices were used for further annealing treatments of thin composite films in the condition of double-sided spatial confinement.

To prepare specimens for transmission electron microscopy (TEM) observations, the annealed samples were etched in a 1 M HCl solution to remove the metal cap and subsequently rinsed in demineralized water several times. The thin composite films were floated off from the substrate onto the surface of demineralized water and transferred to 400 mesh TEM grids.

Devices without top metal layer were used as single-sided confined samples. First, these samples were annealed in contact with the substrate, and subsequently the active layers were transferred to TEM grids as described above. In contrast, for the investigation of free-standing films the active layers were first transferred to TEM grids and then annealed without any contact with a substrate or a top-covering layer.

Annealing of samples was performed under precisely controlled temperature and atmosphere conditions, using a Linkam apparatus (model TMS94) equipped with a THMS600 temperature stage. The samples were kept in a dark chamber with continuous flow of dry argon throughout the entire annealing process to prevent oxidation induced by light, oxygen, and/or water at the high temperature. The stability of the temperature was controlled within 0.1 °C. The annealing experiments were started by rapidly heating (130 °C/min) the samples from room temperature (between 20 and 25 °C) to the desired annealing temperatures. After annealing, the samples were cooled to room temperature at the same rate (130 °C/min).

Transmisstion Electron Microscopy (TEM). Bright-field TEM morphology observations and acquisition of selected-area electron diffraction (SAED) patterns were conducted on a JEOL JEM-2000FX transmission electron microscope operated at 80 kV. Traditional negative plates were used to record all the images. The images were digitized using a negative scanner (Agfa DUO scanner) working in gray mode with 8 bits channel of gray scale. The physical scanning resolution of the negatives was usually between 800 and 1200 dpi.

Atomic Force Microscopy (AFM). AFM investigations of thin composite films after thermal treatment were performed using a Smena P47H, NT-MDT Ltd., Moscow, Russia. The AFM was operated in intermittent-contact mode in air using silicon cantilevers with spring constant k of 11−15 N/m, which were coated with a gold layer for higher laser beam reflectivity. Typical resonance frequencies were 210−230 kHz. The AFM was calibrated using a 25 nm height standard grating produced by NT-MDT Ltd., Moscow, Russia.

Results

As discussed in another study,[7] during spin-coating the solution of MDMO-PPV/PCBM in chlorobenzene, the high rate of solvent evaporation suppresses phase separation. Hence, the spin-coated films are probably not in their equilibrium state, and likely there is a

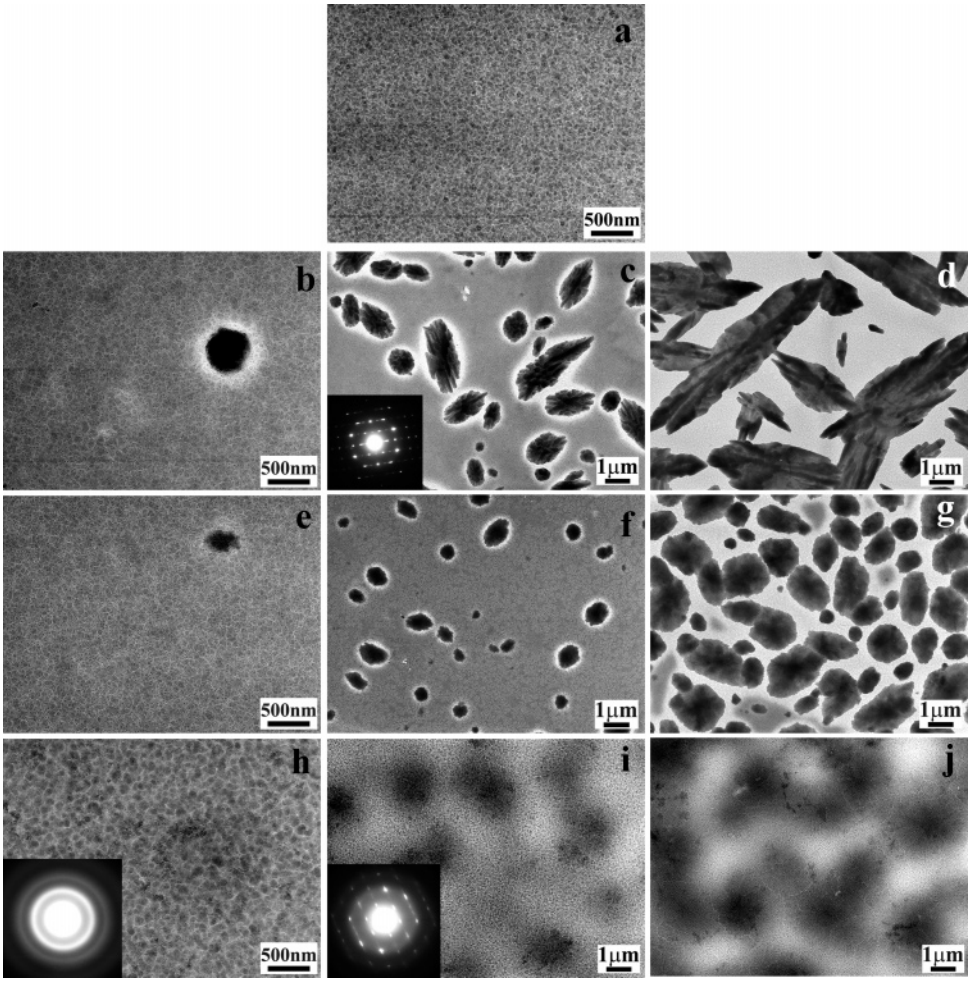

Figure 1. Bright-field TEM images demonstrating the formation of PCBM single crystals with time from MDMO-PPV/PCBM composite films with 80 wt % PCBM upon annealing at 130 °C under different spatial confinements: (a) as spin-coated (fresh) sample; free-standing for (b) 10, (c) 20 and (d) 60 min; single-sided confined for (e) 10, (f) 20, and (g) 60 min; double-sided confined for (h) 20, (i) 38, and (j) 120 min. The insets are corresponding SAED patterns. For double-sided confined films, the metal cap was removed after annealing.

strong thermodynamic driving force to reorganize toward the stable equilibrium state. This process will be accelerated at elevated temperatures and is different for the three types of confinement investigated.

Figure 1 shows bright-field TEM images and corresponding SAED patterns of thin MDMO-PPV/PCBM composite film samples with 80 wt % PCBM. In the TEM images, the darker areas are attributed to PCBM-rich domains because the electron scattering density of PCBM is higher than that of MDMO-PPV.[34] The initial film morphology consists of PCBM nanocrystals homogeneously distributed in the MDMO-PPV matrix (Figure 1a). A more detailed discussion of the interpretation of the diffraction patterns of PCBM can be found in ref 35.

The morphological evolution of the films upon annealing at 130 °C for different types of confinement is monitored. In the case of free-standing film samples, PCBM clusters are formed upon annealing that can be identified in the TEM image as dark areas in a gray MDMO-PPV/PCBM matrix. Notably, the brighter areas surrounding the PCBM clusters reflect thinner regions of the film, being composed of almost pure MDMO-PPV (i.e., depleted from PCBM). We note that the dark PCBM clusters visualized in these images are single crystals, as evidenced from the corresponding SAED pattern (inset in Figure 1c). The PCBM single crystals develop gradually with annealing time and, particularly for these free-standing films, demonstrate a pronounced and highly elongated shape (Figure 1d). The anisotropy of PCBM crystal growth might be related to its asymmetric molecular architecture after decorating naked fullerene C60 with a dissolvable "tail". Notably, the aspect ratio of the single crystals, which is related to the anisotropy of the crystal growth in the lateral dimensions, increases with annealing time from ca. 1.5 (almost circular) at initial stage to 3.5 after 60 min thermal treatment.

For the case of single-sided confinement, a somewhat similar evolution of the morphology of thin film MDMO-PPV/PCBM composites can be followed. PCBM single crystals continuously grow during the annealing process (Figure 1e−g). However, when the thin film samples are supported by a solid substrate (PEDOT:PSS), the PCBM crystals formed are smaller and less elongated as compared with free-standing film samples for the same annealing times. The aspect ratio of the crystals stays constant at approximately 1.5.

In contrast, the morphological evolution of samples in double-sided confinement follows a different route. For an annealing time of 20 min the morphology of the samples seems to be unchanged (Figure 1h). However, the appearance of the PCBM-rich clusters become more prominent, and the size of the clusters is increased from

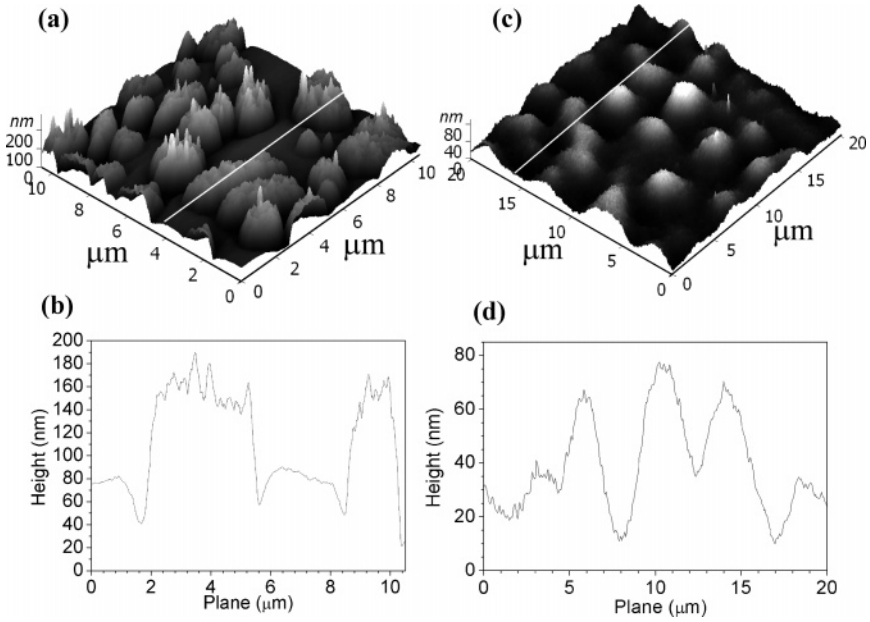

Figure 2. AFM topography images and corresponding cross-sectional profiles for MDMO-PPV/PCBM composite films annealed at 130 °C (a, b) under single-sided confinement for 60 min and (c, d) under double-sided confinement for 120 min. For double-sided confined films, the metal cap was removed after annealing for AFM measurement. Note: the z range for the two topography images is different.

initially ~80 to ~120 nm. Corresponding SAED (Figure 1h inset) analysis has revealed that the clusters are still composed of PCBM nanocrystals.

When the annealing time is increased, further reorganization of the PCBM-rich domains can be observed. Relatively dark regions are emerging from the initially rather homogeneous composite film (Figure 1i,j), which seems to be PCBM crystals. Because of the difference in morphology compared to the PCBM single crystals as introduced above for the cases of free-standing or single-sided confined films, additional SAED analysis was performed. The diffraction pattern (Figure 1i inset) confirms that these dark regions are indeed PCBM single crystals, which still possessing the same crystallographic structure as PCBM crystals formed for the other cases of confinement. Another feature of these crystals is that they have low contrast to the background and their contour is rather fuzzy. A possible reason may be that these PCBM crystals are fairly small in the direction perpendicular to the film plane. However, the lateral size is quite similar compared with those formed from films annealed at single-sided confinement, but they possess almost circular shapes and show no obvious preferred growth direction. It should be noted that the PCBM crystals are not surrounded by a bright halo as introduced for the cases of no or single-sided confinement.

The heights of the PCBM crystals formed during annealing with single- and double-sided confinements have been studied by using atomic force microscopy in intermittent contact mode. Figure 2 shows AFM height images and the corresponding topography scanning curves. The height of PCBM crystals grown during annealing at 130 °C for 60 min in the case of single-sided confinement (Figures 2a,b) is approximately 200 nm. Moreover, from the AFM height scans in Figure 2b it can be observed that the film is thinner around the central PCBM cluster, which confirms that the bright area surrounding the PCBM clusters, as demonstrated by TEM (Figure 1c,f), reflects thinner regions of the composite film being depleted from PCBM. For the PCBM single crystals developed in the double-sided confined films (Figure 2c,d), the height difference within the films is much smaller (~70 nm) compared to that of crystals grown in a single-sided confined film. This result confirms that the thickness of PCBM single crystals formed in severely confined condition, being on the order of the film thickness, is much smaller compared to crystals grown from less confined conditions.

The size of PCBM single crystals grown from the thin composite films during thermal annealing with different confinement conditions are monitored and analyzed. Figure 3 shows a plot of growth rates of crystal dimensions during annealing. The sizes of the crystals are measured in two lateral dimensions: the fast, and thus preferred growth direction of the crystals, and perpendicular to this fast growing direction. The evolution of the aspect ratio (the ratio between lateral dimension in preferred growth direction and growing direction perpendicular to the preferred growth direction, which is here employed to describe the anisotropy of crystal growth for different confinement conditions) with annealing time under different confinements is given in Figure 4. For an easy comparison and to exactly describe the effect of confinement conditions on size and shape of the PCBM crystals, it is assumed that crystal growth is always anisotropic during the annealing experiments. This means that a crystal with a circular shape has an aspect ratio of 1.

As shown in Figure 3a, the crystal sizes in both the fast and slow lateral growth directions in free-standing composite films during annealing can be linearly fitted with annealing time (t), which means a constant growth velocity. For the crystals developed from single-confined composite film, only growth velocity in the slow direction follows this constant. The growth rate in the fast direction, however, can be linearly fitted with square root of annealing time ($t^{1/2}$). For the double-sided confined composite film, the growth rate in both the fast and slow directions follows linear relationship with $t^{1/2}$ (as shown in Figure 3b).

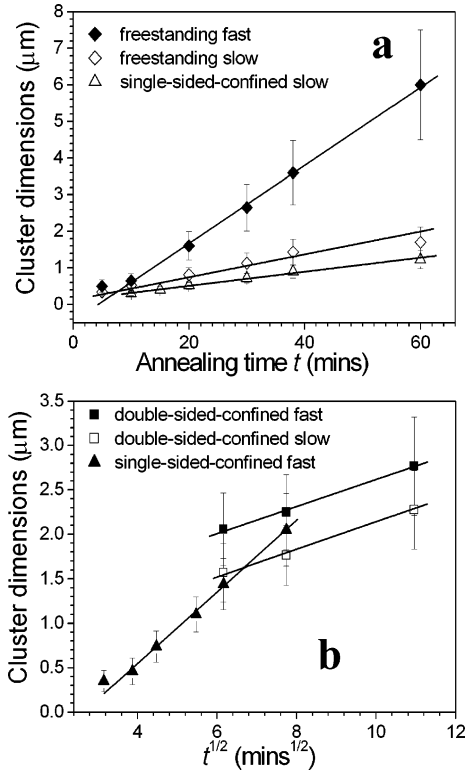

Figure 3. Growth rates of PCBM single crystals from the thin composite films annealed at 130 °C for the various confinements. (a) Cluster dimensions vs annealing time t in the fast (diamond, solid) and slow (diamond, open) growth directions for the free-standing film and in the slow (up-triangle, open) growth direction for the single-sided confined film. (b) Cluster dimensions vs $t^{1/2}$ (t is annealing time) in both the fast (square, solid) and slow (square, open) growth directions for the double-sided confined film and in the fast (up-triangle, solid) growth direction for the single-sided confined film. The solid lines are the linear fitting.

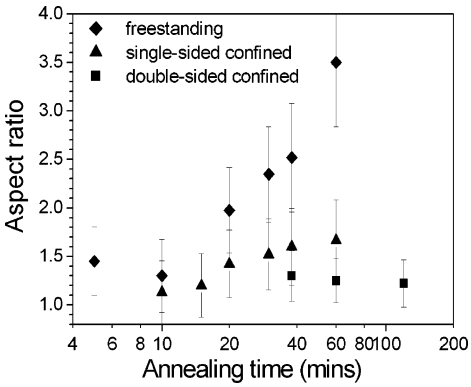

Figure 4. Aspect ratio evolution of PCBM single crystals vs annealing time under various spatial confinements for thin composite films annealed at 130 °C.

Discussion

The kinetics of PCBM crystal growth in thin composite films is controlled by long-range diffusion of PCBM molecules through the polymer matrix to the specific crystal growth fronts and by the local incorporation rate of PCBM molecules into the growing crystals. In contrast to gaseous molecules, where gas transport is one of hopes of ~1.0 nm between cavities existing in the polymer matrix,[28] the translational diffusion of relatively bulky organic compounds such as PCBM, however, is expected to carry out through significant coupling with the dynamic of conformational changes of the polymer host. Typically, the diffusion of these organic molecules in amorphous polymers is favored and can be interpreted in terms of the free volume theory. Using this approach, the kinetics of PCBM diffusion through the MDMO-PPV matrix is associated with the relaxation or motion of MDMO-PPV molecules. On the other hand, local assembling of the PCBM molecules at the growth fronts primarily depend on the interfacial free energy difference between the surrounding matrix and the growing crystal and additional structural considerations such as the crystallographic orientation of the growth fronts. Therefore, the PCBM crystal growth kinetics is actually determined either by the limitation of conformational dynamics of the MDMO-PPV molecules or by the local molecule incorporation rate in the specific crystallographic planes at the crystal growth front.

Since MDMO-PPV is an amorphous polymer, its conformational relaxation upon annealing should be isotropic, at least in the lateral directions within the composite film. Correspondingly, it is expected that the diffusion of PCBM molecules through the MDMO-PPV matrix is isotropic within the lateral plane of the film. However, as shown in Figure 1b−d for the case of a free-standing composite film without confinement, the PCBM crystals are elongated. This morphological feature can be associated with an anisotropic growth behavior of the PCBM crystals: the incorporation rate of PCBM molecules at the two growing directions of the crystal is different, which eventually means that the growth of the PCBM crystals is rather controlled by the integration of free PCBM molecules into its crystals at the crystal growth fronts than by the diffusion of PCBM molecules within the polymer matrix. This unperturbed crystal growth kinetics is further confirmed by the constant growth rate with annealing time in both the fast and slow directions.[36] Therefore, the diffusion rate of the PCBM molecules is higher than their incorporation rate at the crystal growth fronts, which means that

$$R_{\text{diffusion}} > R_{\text{incorporation-fast}} \quad (1)$$

where $R_{\text{diffusion}}$ denotes to the lateral diffusion rate of PCBM molecules within the polymer matrix and $R_{\text{incorporation-fast}}$ to the crystal growth rate in the fast growing direction.

With more confinement exerted to the composite films during annealing, the growth rate of the PCBM crystals in the fast growth direction is reduced, while the growth rate in the slow growth direction seems to be similar compared with the condition of nonconfinement. Obviously, this behavior is related to the lower diffusion rate of PCBM molecules within the polymer matrix for this condition of confinement. The confinement causes the retarded conformational dynamics of the host polymer chains and thus the diffusion rate of PCBM molecules within polymer matrix. Since the crystal growth rate in a diffusion-limited system usually shows a power law annealing time dependence with power 0.5,[37] i.e., $L \propto t^{1/2}$. The linear relationship of crystal growth rate with $t^{1/2}$ in the fast direction reveals the diffusion-limited crystallization, which eventually means the diffusion of PCBM is lower than its incorporation rate at the fast crystal growth direction. In contrast, the constant growth rate with time in the slow growth direction shows that the kinetics of crystal growth in this plane has not been perturbed, and the diffusion rate of PCBM

is still higher than the incorporation rate at the slow growth plane. Thus, it has

$$R_{\text{incorporation-slow}} < R_{\text{diffusion}} < R_{\text{incorporation-fast}} \quad (2)$$

where $R_{\text{incorporation-slow}}$ denotes the crystal growth rate in the slow direction. In such a case, the diffusion rate of PCBM molecules within the polymer matrix controls at least the growth rate of the fast growing direction of PCBM crystals. Thus, the aspect ratio of crystals grown from single-sided confinement is lower compared to crystals grown without presence of confinement condition.

Finally, when the composite film is sandwiched or double-sided confined, only PCBM crystals with rather round shapes are formed during annealing. As shown in Figure 4, the aspect ratios of crystals formed in this confinement condition are constant and close to 1. The growth rate of the fast crystal growth direction is further reduced and equal to the growth rate of the slow growth direction, while the latter seems to be similar compared with the growth rates for the conditions of non- or single-sided confinement. Therefore, for the case of double-sided confinement, the diffusion rate of PCBM molecules within the matrix and the incorporation rates in both directions at crystal growth fronts become equivalent. The crystal growth rates in all directions are diffusion-limited (as shown in Figure 3b). Accordingly, there has

$$R_{\text{diffusion}} \sim R_{\text{incorporation-slow}} < R_{\text{incorporation-fast}} \quad (3)$$

As mentioned above, the mobility of polymer chains in free-standing thin films appears to enhance, as indicated by suppression of the film's apparent T_g. This has encouraged the speculation of a highly mobile, low-viscosity and low-density layer close to free surface that contributes to a reduction of the apparent T_g. The reduced T_g improves the dynamics of polymer chains within this thin film, which benefits the diffusion of PCBM molecules within the polymer matrix. In contrast, in the case of a thin composite polymer film is directly contacted with an impenetrable interface such as a solid substrate, the mobility of polymer chains close to the interface is likely to decrease through a reduction in conformational entropy, which is related to 2-fold reasons. One is that the strong positive interaction between the polymer and substrate will "tie" portions of the chain to the interface.[31,38] Moreover, an impenetrable interface limits the free volume, which spatially prevents the mobility of polymer chains, and thus the diffusion of PCBM molecules. More detailed work concerning this part will be discussed in another study.[39]

For a ready-to-work device, the morphologically thermal stability of the active layer is determined by the T_g of the bulk composite due to the presence of double-sided confined condition, where no free surface exists that can enhance the conformational dynamics of the host polymer and thus the mobility of guest molecules. Therefore, for a composite film consisting of one polymer and other small-molecular organic compounds, how to design this composite with high T_g is quite important for the thermal and long-term stability of the whole photoactive layer. For the active layers only containing polymers, where the interdiffusion between two or even more polymer constitutes could happen and thus the glass transition temperature of each polymer has an equivalent impact on the morphological stability of these active layers.

Conclusion

The morphology evolution of thin molecules/conjugated polymer composite films as used for photovoltaic or pLEDs applications is critical for the performance and lifetime of the real devices. As an example, we present the results based on thin MDMO-PPV/PCBM composite films, which are currently used as photoactive layer in a plastic solar cell. The morphology evolution of the film upon thermal annealing is monitored under various spatially confined conditions.

For all the confinement conditions, large-scale crystallization of PCBM from the composite films is observed in the case of annealing temperatures above the T_g of bulk polymer. Elongated shapes of PCBM crystals are observed, preferably for the free-standing films. The crystal growth rate for this case is determined by the incorporation rate of PCBM molecules at the growth fronts instead of diffusion within the matrix. As more confinement is exerted to the composite film during annealing, the diffusion rate of PCBM molecules within the matrix is reduced and sets in determining the crystal growth rate. Therefore, less elongated and even round PCBM crystals are obtained for single- and double-sided confined films, respectively.

As a potential method to control the morphology of the photoactive layer in an optoelectronic device, post-thermal treatment should be performed with an appropriate condition. Notably temperature and time should be prudently chosen so as molecules/polymer chains in photoactive layer are able to reorganize effectively toward the optimum morphology with a maximum improvement for device performance. At the same time, annealing treatment should not exceed critical limitation and induce further change (for example, interface damage with electrode was observed for an annealing time of 120 min) in the devices. In another aspect study for the stabilizing an achieved morphology for a photoactive layer in photoactive or pLED applications, we ultimately expect to find a solution that will allow the creation of this composite layer, which possesses long-term morphological stability during real operation, without a decrease in performance.

Acknowledgment. The work of X.Y. forms part of the research program of the Dutch Polymer Institute (DPI project #326). We thank Prof. R. A. J. Janssen for helpful discussions, Dr. J. K. J. van Duren for assistance in sample preparation, and Dr. Mingwen Tian (NT-MDT Europe) for a part of the AFM measurements. We also pay our appreciation to Prof. J. C. Hummelen and Dr. M. T. Rispens for a generous gift of PCBM and to Philips for a generous gift of MDMO-PPV.

References and Notes

(1) Ditmer, J. J.; Marsegla, E. A.; Friend, R. H. *Adv. Mater.* **2000**, *12*, 1270.
(2) Camaioni, N.; Ridolfi, G.; Casalbore-Miceli, G.; Possamai, G.; Maggini, M. *Adv. Mater.* **2002**, *14*, 1735.
(3) Cabanillas-Gonzalez J.; Yeates, S.; Bradley, D. D. C. *Synth. Met.* **2003**, *139*, 637.
(4) Padinger, F.; Rittberger, R. S.; Sariciftci, N. S. *Adv. Funct. Mater.* **2003**, *13*, 85.
(5) Peumans, P.; Uchida, S.; Forrest, S. R. *Nature (London)* **2003**, *425*, 158.

(6) Chirvase, D.; Parisi, J.; Hummelen, J. C.; Dyakonov, V. *Nanotechnology* **2004**, *15*, 1317.
(7) Yang, X. N.; van Duren, J. K. J.; Janssen, R. A. J.; Michels, M. A. J.; Loos, J. *Macromolecules* **2004**, *37*, 2151.
(8) Hoppe, H.; Niggemann, M.; Winder, C.; Kraut, J.; Hiesgen, R.; Hinsch, A.; Meissner, D.; Sariciftci. N. S. *Adv. Funct. Mater.* **2004**, *14*, 1005.
(9) Kroon, J. M.; Wienk, M. M.; Verhees, W. J. H.; Hummelen, J. C. *Thin Solid Films* **2002**, *403*−*204*, 223.
(10) Fujita, H. *Adv. Polym. Sci.* **1961**, *3*, 1.
(11) Vrentas, J. S.; Duda, J. L.; Ling, H.-C. *J. Polym. Sci., Polym. Phys. Ed.* **1985**, *23*, 275.
(12) Hall, D. B.; Torkelson, J. M. *Macromolecules* **1998**, *31*, 8817.
(13) Tseng, K. C.; Turro, N. J.; Durning, C. J. *Phys. Rev. E* **2000**, *61*, 1800.
(14) Vyprachticky, D.; Morawetz, H.; Fainzilberg, V. *Macromolecules* **1993**, *26*, 339.
(15) Smith, B. A. *Macromolecules* **1982**, *15*, 469.
(16) Byers, G. W. *Macromolecules* **1993**, *26*, 4242.
(17) Ogawa, T.; Nagata, T.; Hamada, Y. *J. Appl. Polym. Sci.* **1993**, *159*, 243.
(18) Cicerone, M. T.; Blackburn, F. R.; Ediger, M. D. *Macromolecules* **1995**, *28*, 8224.
(19) Deppe, D. D.; Dhinojwala, A.; Torkelson, J. M. *Macromolecules* **1996**, *29*, 3898.
(20) Forrest, J. A.; Dalnoki-Veress, K.; Dutcher, J. R. *Phys. Rev. E* **1997**, *56*, 5705.
(21) Frank, B.; Gast, A. P.; Russell, T. P.; Brown, H. R.; Hawker, C. *Macromolecules* **1996**, *29*, 6531.
(22) Reiter, G. *Europhys. Lett.* **1993**, *23*, 579 and references therein.
(23) Zhao, W.; Zhao, X.; Rafailovich, M. H.; Sokolov, J.; Komposto, R. J.; Smith, J. J.; Dozier, W. D.; Mansfield, J.; Russell, T. P. *Macromolecules* **1993**, *26*, 561.
(24) Mayes, A. M. *Macromolecules* **1994**, *27*, 3114.
(25) Tanaka, K.; Taura, A.; Ge, S.; Takahara, A.; Kajiyama, T. *Macromolecules* **1996**, *29*, 3040.
(26) Forrest, J. A.; Dalnoki-Veress, K.; Stevens, J. R.; Dutcher, J. R. *Phys. Rev. Lett.* **1996**, *77*, 2002.
(27) Toney, M. F.; Russell, T. P.; Logan, J. A.; Kikuchi, H.; Sands, J. M.; Kumar, S. K. *Nature (London)* **1995**, *374*, 709.
(28) Gusev, A. A.; Suter, U. W. *J. Chem. Phys.* **1993**, *99*, 2228.
(29) Liu, Y.; Russell, T. P.; Samant, M. G.; Stöhr, J.; Brown, H. R.; Cossy-Favre, A.; Diaz, J. *Macromolecules* **1997**, *30*, 7768.
(30) Ge, S.; Pu, Y.; Zhang, W.; Rafailovich, M.; Sokolov, J. *Phys. Rev. Lett.* **2000**, *85*, 2340.
(31) Wallace, W. E.; van Zanten, J. H.; Wu, W. L. *Phys. Rev. E* **1995**, *52*, 3329.
(32) Orts, W. J.; van Zanten, J. H.; Wu, W. L.; Satija, S. K. *Phys. Rev. Lett.* **1993**, *71*, 867.
(33) van Duren, J. K. J.; Yang, X. N.; Loos, J.; Bulle-Lieuwma, C. W. T.; Sieval, A. B.; Hummelen, J. C.; Janssen, R. A. J. *Adv. Funct. Mater.* **2004**, *14*, 425.
(34) Bulle-Lieuwma, C. W. T.; van Gennip, W. J. H.; van Duren, J. K. J.; Jonkheijm, P.; Janssen, R. A. J.; Niemantsverdriet, J. W. *Appl. Surf. Sci.* **2003**, *203*−*204*, 547.
(35) Yang, X. N.; van Duren, J. K. J.; Rispens, M. T.; Hummelen, J. C.; Janssen, R. A. J.; Michels, M. A. J.; Loos, J. *Adv. Mater.* **2004**, *16*, 802.
(36) Chernov, A. A. *Modern Crystallography III Crystal Growth*; Springer Series Solid State Vol. 36; Springer: Berlin, 1984.
(37) Yamakawa, H. *Modern Theory of Polymer Solutions*; Harper and Row: New York, 1971.
(38) Kuhlmann, T.; Kraus, J.; Müller-Buschbaum, P.; Schubert, D. W.; Stamm, M. *J. Non-Cryst. Solids* **1998**, *235*, 457.
(39) Yang, X. N.; Tian, M. W.; Michels, M. A. J.; Loos, J.; et al. To be published.

MA047589X